# Scleraxis-Targeted Deletion of Non-Muscle Myosin Leads to Tendon Degeneration

Mary Kate Evans[1], Tonia K. Tsinman[1], Ellie Ferguson[1], Xi Jiang[1], Joel Boerckel[1], Lin Han[2], Eiki Koyama[3], Robert L. Mauck[1], Nathaniel A. Dyment[1]
[1]University of Pennsylvania, [2]Drexel University, and [3]Children's Hospital of Philadelphia, Philadelphia, PA
mkevans@seas.upenn.edu

**Disclosures**: RL Mauck (4, Mechano Therapeutics, 5, 4Web Medical, *8, JOR Spine*), No other disclosures.

**INTRODUCTION**: The specific mechanisms that regulate tendon cell response to externally applied mechanical loads during tendon growth, homeostasis, and healing are not well understood, resulting in large variation in both physical therapy regimens and patient response to treatment for tendon pathologies [1]. To better understand the cell-intrinsic mechanisms that regulate tendon adaptation to applied loads, we investigated actomyosin contractility, which relies on the interaction of non-muscle myosin (NM-II) motor proteins and actin filaments to generate contractile force and transduce signals from applied loads to the nucleus [2]. Prior *ex vivo* studies demonstrated that NM-II mediated contractility can regulate matrix remodeling [3-4] via YAP/TAZ signaling [5]. Yet, the importance of actomyosin contractility in tendon formation and maintenance *in vivo* is unknown. Therefore, we ablated NM-II proteins in tendons throughout growth and development. We hypothesized that NM-II regulates cell and matrix organization in a cell-autonomous fashion and is required to maintain tissue homeostasis.

**METHODS:** All animal work was IACUC approved. Mouse Model: To preferentially ablate NM-II in tendons, we targeted the predominant NM-II isoforms, NM-IIA (*Myh9* gene) and NM-IIB (*Myh10* gene) using the Scleraxis (Scx) Cre driver to generate ScxCre;Myh9$^{f/f}$;Myh10$^{f/f}$ mice (myosin dKO) and Cre-negative littermate controls (WT). Cryohistology: Knees and ankles from P2, P28, and P112 myosin dKO and WT mice were fixed and sectioned in the sagittal plane. *In Situ* Hybridization (ISH): P2 patellar tendon sections (n=2-3/group) were stained for *Myh9* (C1) and *Myh10* (C2) RNA using the BaseScope Duplex Assay. Cytoskeletal Organization: F-actin (phalloidin staining) with cell nuclei were visualized via confocal z-stacks in P28 patellar tendon sections (n=3/group). Alignment was assessed in FIJI using the OrientationJ plugin. Tendon Morphology: P28 and P112 sections (n=4-7/group) were stained and imaged in two rounds: (1) calcein blue (CB), alkaline phosphatase (ALP), and TO-PRO-3 (nuclei), (2) Toluidine Blue, and were used to determine patellar tendon length and nuclear aspect ratio. Gene Expression: Patellar and Achilles tendon tissue sections (n=4-5/group) were collected for qPCR using a Standard BioTools Dynamic Array for 96 genes of interest. Statistics: Groups were compared via one-way ANOVA with Tukey post-hoc tests (α=0.05).

**RESULTS:** NM-II knockdown disrupts cytoskeletal organization. ISH confirmed knockdown of *Myh9* and *Myh10* and highlighted a subset of high-expressing cells, which may be non scx-lineage cells (i.e., macrophages) or cells that did not undergo Cre-mediated ablation of *Myh9* and *Myh10* (**Fig. 1A**). By P28, NM-II knockdown resulted in regions of disorganized actin cytoarchitecture (**Fig. 1B**). Myosin dKO tendons display degenerative features in adulthood. At P112, this cellular disorganization progressed to degeneration with an elongated tendon (**Fig. 2C**) containing cells with reduced nuclear aspect ratio (**Fig. 2D**) and a disorganized matrix with increased proteoglycan staining (**Fig. 2A-B**). In fact, ectopic mineralization was evident in 4/6 patellar and 5/5 Achilles tendons in myosin dKO mice, compared to 0% in WT tendons. Expression profile of myosin dKO tendons suggest increased remodeling. Finally, gene expression analyses and hierarchical clustering revealed a marked difference in gene expression between WT and myosin dKO mice at both P28 and P112, with increased expression of both anabolic (e.g., *Col1a1*, *Col3a1*, *Lox*) and catabolic markers (e.g., *Mmp13*, *Mmp14*, *Timp1*) in myosin dKO tendons, with these changes being more pronounced in the patellar tendon than the Achilles (**Fig. 3**).

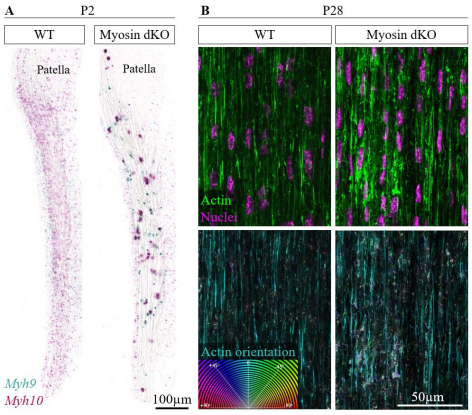


**Fig 1: Disrupted cytoskeleton from NM-II ablation**. (A) *Myh9* (green) and *Myh10* (red) *in situ* hybridization staining. (B) Maximum intensity projections of nuclei and actin (top) and actin orientation (bottom).

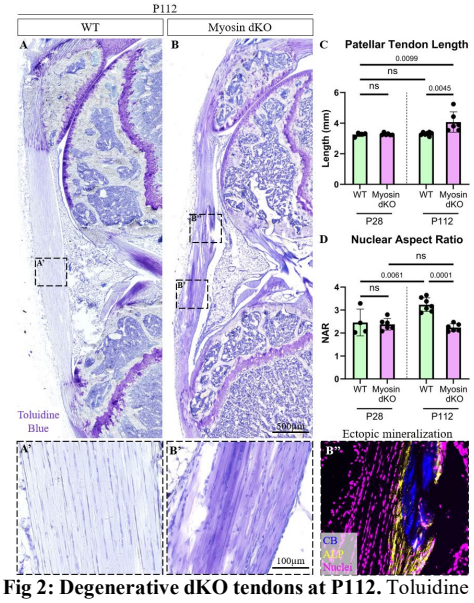


**Fig 2: Degenerative dKO tendons at P112.** Toluidine Blue (A-B), calcein blue (CB, B'') for mineral, and alkaline phosphatase (ALP, B'') staining. Elongated PTs (C) with decreased nuclear aspect ratio (D) in P112 myosin dKO tendons that is not present at P28.

**DISCUSSION**: This study highlights the progressive onset of tendon degeneration following sustained ablation of *Myh9* and *Myh10* throughout tendon growth and development. Although P28 myosin dKO tendons display differences in actin organization and gene expression, they do not yet display the patellar tendon elongation and decreased nuclear aspect ratio present at P112. This progressive onset of tendon degeneration may parallel what has been shown *ex vivo*, where a disruption in tensional homeostasis can trigger a catabolic response and aberrant matrix remodeling [3-5]. Additionally, it is possible that disrupted actomyosin contractility impairs the ability of tenocytes to sustain the increased loading demands leading into adulthood. Alternatively, it may be that, once tendon cells mature and establish a tensional homeostatic set point required for proper tissue maintenance, the cells are less capable of responding appropriately to altered loading. These mechanisms could explain the failure of nuclear elongation and increased tissue disorganization with age as the phenotype progressively worsens; however, investigation at intermediate timepoints is still necessary.

**SIGNIFICANCE:** Establishing how actomyosin contractility regulates tendon cell response to applied loads throughout tissue development and maturation will inform the pathogenesis of tendon disease and potentially inform future treatments.

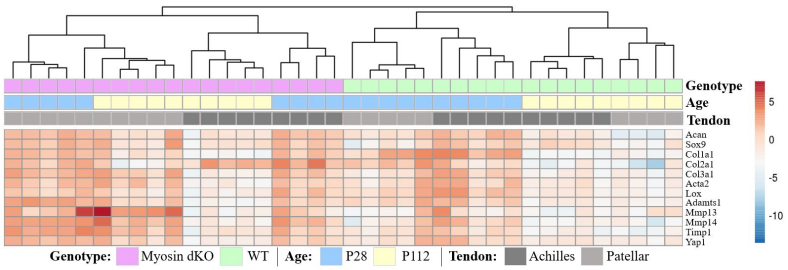


**Fig 3: Increased anabolic/catabolic expression in dKO tendons.** Heatmap and hierarchical clustering for subset of genes (12 from 91 total) from qPCR array.

**REFERENCES:** 1. Galloway, *J Bone Joint Surg*, 2013; 2. Franke, *Curr Biol*, 2005; 3. Schiele, *JOR*, 2015; 4. Arnoczky, *JOR,* 2004; 5. Jones, *PNAS*, 2023.
**ACKNOWLEDGEMENTS:** Work was supported by NIH P50 AR080581, P30 AR069619, R01 AR075418, T32 AR007132, and VA IK6 RX003416.